Event-by-event charged-neutral fluctuations in Pb plus Pb collisions at 158 A GeV

Aggarwal, M. M.; Ahammed, Z.; Angelis, A. L. S.; Antonenko, V.; Arefiev, V.; Astakhov, V.; Avdeitchikov, V.; Awes, T. C.; Baba, P. V. K. S.; Badyal, S. K.

Published in:
Physics Letters B

DOI:
10.1016/j.physletb.2011.06.003

Physics Letters B 701 (2011) 300–305

Contents lists available at ScienceDirect

Physics Letters B

www.elsevier.com/locate/physletb

Event-by-event charged–neutral fluctuations in Pb + Pb collisions at 158 *A* GeV

WA98 Collaboration

M.M. Aggarwal[a], Z. Ahammed[b], A.L.S. Angelis[c,1], V. Antonenko[d], V. Arefiev[e], V. Astakhov[e], V. Avdeitchikov[e], T.C. Awes[f], P.V.K.S. Baba[g], S.K. Badyal[g], S. Bathe[h], B. Batiounia[e], T. Bernier[i], K.B. Bhalla[j], V.S. Bhatia[a], C. Blume[h], D. Bucher[h], H. Büsching[h], L. Carlen[k], S. Chattopadhyay[b], M.P. Decowski[l], H. Delagrange[i], P. Donni[c], M.R. Dutta Majumdar[b], K. El Chenawi[k], A.K. Dubey[b], K. Enosawa[n], S. Fokin[d], V. Frolov[e], M.S. Ganti[b], S. Garpman[k,1], O. Gavrishchuk[e], F.J.M. Geurts[o], T.K. Ghosh[b], R. Glasow[h], R. Gupta[g], B. Guskov[e], H.Å. Gustafsson[k,1], H.H. Gutbrod[q], I. Hrivnacova[r], M. Ippolitov[d], H. Kalechofsky[c], R. Kamermans[o], K. Karadjev[d], K. Karpio[s], B.W. Kolb[q], I. Kosarev[e], I. Koutcheryaev[d], A. Kugler[r], P. Kulinich[l], M. Kurata[n], A. Lebedev[d], H. Liu[s], H. Löhner[p], L. Luquin[i], D.P. Mahapatra[m], V. Manko[d], M. Martin[c], G. Martínez[i], A. Maximov[e], Y. Miake[n], G.C. Mishra[m], B. Mohanty[b], M.-J. Mora[i], D. Morrison[t], T. Moukhanova[d], D.S. Mukhopadhyay[b], H. Naef[c], B.K. Nandi[m], S.K. Nayak[g], T.K. Nayak[b], A. Nianine[d], V. Nikitine[e], S. Nikolaev[d], P. Nilsson[k], S. Nishimura[n], P. Nomokonov[e], J. Nystrand[k], A. Oskarsson[k], I. Otterlund[k], S. Pavliouk[d], T. Peitzmann[o], D. Peressounko[d], V. Petracek[r], W. Pinanaud[i], F. Plasil[f], M.L. Purschke[q], J. Rak[r], R. Raniwala[j], S. Raniwala[j], N.K. Rao[g], F. Retiere[i], K. Reygers[h], G. Roland[l], L. Rosselet[c], I. Roufanov[e], C. Roy[i], J.M. Rubio[c], S.S. Sambyal[g], R. Santo[h], S. Sato[n], H. Schlagheck[h], H.-R. Schmidt[q], Y. Schutz[i], G. Shabratova[e], T.H. Shah[g], I. Sibiriak[d], T. Siemiarczuk[s], D. Silvermyr[k], B.C. Sinha[b], N. Slavine[e], K. Söderström[k], G. Sood[a], S.P. Sørensen[t], P. Stankus[f], G. Stefanek[s], P. Steinberg[l], E. Stenlund[k], M. Sumbera[r], T. Svensson[k], A. Tsvetkov[d], L. Tykarski[s], E.C.v.d. Pijll[o], N.v. Eijndhoven[o], G.J.v. Nieuwenhuizen[l], A. Vinogradov[d], Y.P. Viyogi[b,*], A. Vodopianov[e], S. Vörös[c], B. Wysłouch[l], G.R. Young[f]

[a] *University of Panjab, Chandigarh 160014, India*
[b] *Variable Energy Cyclotron Centre, Calcutta 700 064, India*
[c] *University of Geneva, CH-1211 Geneva 4, Switzerland*
[d] *RRC Kurchatov Institute, RU-123182 Moscow, Russia*
[e] *Joint Institute for Nuclear Research, RU-141980 Dubna, Russia*
[f] *Oak Ridge National Laboratory, Oak Ridge, TN 37831-6372, USA*
[g] *University of Jammu, Jammu 180001, India*
[h] *University of Münster, D-48149 Münster, Germany*
[i] *SUBATECH, Ecole des Mines, Nantes, France*
[j] *University of Rajasthan, Jaipur 302004, Rajasthan, India*
[k] *Lund University, SE-221 00 Lund, Sweden*
[l] *MIT Cambridge, MA 02139, USA*
[m] *Institute of Physics, 751-005 Bhubaneswar, India*
[n] *University of Tsukuba, Ibaraki 305, Japan*
[o] *Universiteit Utrecht/NIKHEF, NL-3508 TA Utrecht, The Netherlands*
[p] *KVI, University of Groningen, NL-9747 AA Groningen, The Netherlands*
[q] *Gesellschaft für Schwerionenforschung (GSI), D-64220 Darmstadt, Germany*
[r] *Nuclear Physics Institute, CZ-250 68 Rez, Czech Republic*
[s] *Soltan Institute for Nuclear Studies, PL-00-681 Warsaw, Poland*
[t] *University of Tennessee, Knoxville, TN 37966, USA*

* Corresponding author.
E-mail address: viyogi@vecc.gov.in (Y.P. Viyogi).

[1] Deceased.

0370-2693/$ – see front matter
doi:10.1016/j.physletb.2011.06.003

ARTICLE INFO

Article history:
Received 12 March 2011
Received in revised form 30 May 2011
Accepted 1 June 2011
Available online 7 June 2011
Editor: V. Metag

Keywords:
The WA98 experiment
Photon multiplicity detector
Disoriented chiral condensate
Silicon pad multiplicity detector
Sliding window method
Charged–neutral fluctuations

ABSTRACT

Charged particles and photons have been measured in central Pb + Pb collisions at 158 A GeV in a common (η–ϕ)-phase space region in the WA98 experiment at the CERN SPS. The measured distributions have been analyzed to quantify the frequency with which phase space regions of varying sizes have either small or large neutral pion fraction. The measured results are compared with VENUS model simulated events and with mixed events. Events with both large and small charged–neutral fluctuations are observed to occur more frequently than expected statistically, as deduced from mixed events, or as predicted by model simulations, with the difference becoming more prominent with decreasing size of the $\Delta\eta$–$\Delta\phi$ region.

Enhanced fluctuation in the production of neutral versus charged pions has been one of the predicted signals for chiral symmetry restoration in heavy ion collisions at ultra-relativistic energies [1]. It has been proposed that the extreme energy density of the matter produced in the region of spatial overlap between two heavy ions colliding at relativistic energies may provide the physical conditions necessary for the formation of a chiral condensate that may be aligned in a direction different from the true vacuum. Domains of such Disoriented Chiral Condensates (DCCs) are expected to emit pions coherently from the collision volume, which may result in large fluctuations in the neutral pion fraction, f, defined as $f = N_{\pi^o}/(N_{\pi^o} + N_{\pi^\pm})$, where N_{π^o} and $N_{\pi^\pm}$ are the multiplicities of the neutral and charged pions, respectively. The neutral pion fraction f for DCC domains is predicted to follow a probability distribution of the form $P(f) = 1/2\sqrt{f}$ [2], which is very different from the binomial distribution observed for generic pion production in hadron collisions.

Events with large charged–neutral fluctuations, the so called Centauro ($N_{ch} \gg N_\gamma$) and Anti-Centauro ($N_\gamma \gg N_{ch}$) events, were first observed in the JACEE cosmic ray experiment [3]. The search for such unusual events and DCC formation was later carried out by the D0 [4], CDF [5], and Minimax [6] experiments in p + p collisions at the Tevatron and by the NA49 [7] and WA98 [10–12] experiments in nuclear collisions at the CERN SPS. Upper limits to the production of DCC domains have been set within various model assumptions. WA98 has conducted an exhaustive search for charged–neutral fluctuations in nuclear collisions. In the first WA98 analysis [10], correlated neutral *vs.* charged particle fluctuations were investigated globally over a large η–ϕ acceptance of more than one unit of rapidity near mid-rapidity, with full azimuthal coverage. Subsequent investigations based on statistical correlations [11] or multi-resolution Discrete Wavelet Transform (DWT) techniques [12], searched for DCC-like fluctuations in localized regions of (η–ϕ) phase space.

In this Letter we present an improved search for localized charged–neutral fluctuations in central Pb+Pb collisions at the SPS using a simple Sliding Window Method (SWM) [13]. This method utilizes the azimuthal resolution of the WA98 detectors to identify all regions with unusually large or small values of the neutral particle fraction. The sensitivity of the SWM has been studied using simulated data based on simple model assumptions of charged–neutral fluctuations similar to those used in the study of the DWT method [11,14]. The SWM is found to have a sensitivity which is limited only by the available statistics and can be several orders of magnitude better than the DWT method for a given data sample. Preliminary results have been presented in Refs. [15,16].

The analysis reported here used the measurement of photons and charged particles produced in Pb + Pb collisions at 158 A GeV recorded by the WA98 experiment, during a period of magnetic field-off operation of WA98 in the 1996 run period of the CERN SPS. Photons were measured with the Photon Multiplicity Detector (PMD) [9] and charged particles were measured with the Silicon Pad Multiplicity Detector (SPMD) [8]. The analysis is restricted to their common region of η–ϕ acceptance overlap. The PMD was located at 21.5 meters downstream of the target and consisted of plastic scintillator pads of varying sizes arranged inside 22 box modules placed behind $3X_0$ thick lead converter plates [9]. It covered the pseudorapidity region $2.9 < \eta < 4.2$. For the photon identification criteria applied the average photon counting efficiency and the purity of the photon sample were found to be 68% and 65%, respectively, for the central event sample used [17]. The azimuthal resolution of the PMD is much less than 1° and the limit for detection of low p_T particles is 30 MeV/c. The SPMD was located at 32.8 cm from the target and consisted of 22 radial and 46 azimuthal segments in each of four quadrants. It covered the pseudorapidity region of $2.35 < \eta < 3.75$ [8]. The charged particle detection efficiency of the SPMD was 99%. The azimuthal resolution of the SPMD is 2° and the limit for detection of low p_T particles is nearly zero. The total transverse energy E_T measured in the pseudorapidity region $3.5 < \eta < 5.5$ by the Midrapidity Calorimeter (MIRAC) [18], located 24 m downstream of the target, was used to characterize the event centrality. All procedures for event selection and removal of backgrounds described in detail in previous publications [11,12,15,17] were followed in the present analysis. A total of 185 K events, belonging to the 15% most central collisions of the WA98 minimum bias data sample, with the WA98 field-off minimum bias cross-section measured to be 6.2 b, have been analyzed.

In the present analysis, the multiplicity of photons measured in the PMD and the multiplicity of charged particles measured in the SPMD, in the region of common η acceptance ($2.9 < \eta < 3.75$), are employed as experimental observables to approximate the neutral pion fraction by the neutral particle fraction $f \approx \frac{N_\gamma/2}{N_\gamma/2+N_{ch}}$. The neutral particle fraction f is calculated within windows of varying size $\Delta\phi$ in azimuth.

The search for non-statistical fluctuations requires comparison with a model-independent baseline, free of dynamical correlations, that includes detector effects and fluctuations of statistical nature only. For the analysis of experimental data the technique of event-mixing can provide such a reference data sample in which dynamical correlations among particles are completely destroyed, leaving only correlations that might result from efficiency variations. The mixed events are generated by the standard procedure of using real events to construct new mixed events with particles selected randomly, one particle per real event. In this analysis, the mixed events are created with the same multiplicity distribution as the

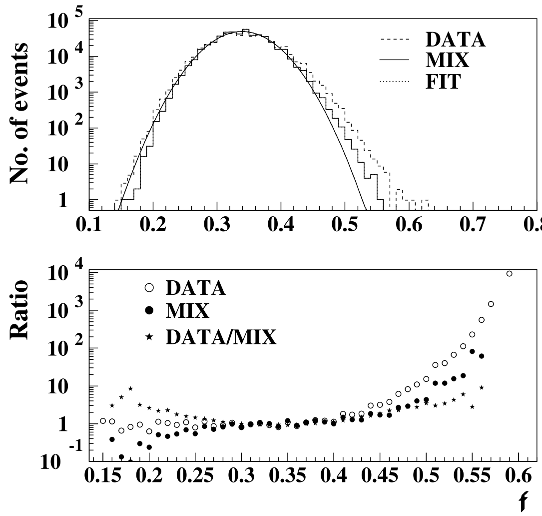

Fig. 1. Top: The f distributions for data and mixed events for the 5% most central Pb + Pb events for randomly selected η–ϕ regions with $\Delta\phi = 60°$. A fit to the distribution for mixed events with a Gaussian function, with fit parameters mean $= 0.33923 \pm 0.00004$ and $\sigma = 0.04041 \pm 0.00004$, is also shown. Bottom: Ratio of the f distributions for the data and the Gaussian fit to the mixed events (open circles) and the ratio of the mixed events with its Gaussian fit (solid circles). Ratio of data to mixed events is also shown for comparison.

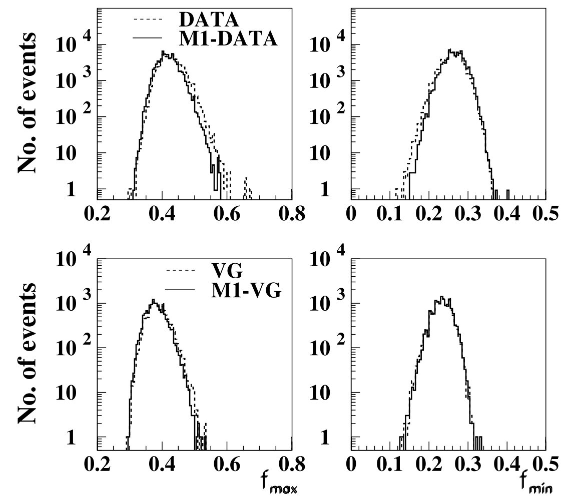

Fig. 2. The f_{max} (left) and f_{min} (right) distributions for $\Delta\phi = 60°$ window size for data (top) and VG (bottom) for the 5% most central events together with the distributions for their respective mixed events.

experimental data. Furthermore, for each real event, a mixed event is created with the same charged particle and photon hit multiplicity, thereby maintaining the same charged–neutral multiplicity correlation. Two kinds of mixed events are used in this study [12]. In the first case, termed M1 mixed (or maximally mixed) events, all of the charged particle and neutral hits in each mixed event are selected from different real events. Thus the M1 mixed events constitute fully mixed events with only the global charged–neutral multiplicity correlation maintained. The second class of artificial events, termed M2 mixed (or minimally mixed) events [12], are created by mixing PMD and SPMD subevents from different events, but without mixing hits within the individual detectors. In the M2 mixed events the charged and neutral fluctuations are separately maintained, but the correlation between charged and neutral hits is removed, except that the global charged–neutral multiplicity correlation is maintained. In what follows the mixed events are the M1 type unless explicitly stated.

Two approaches have been used to characterize the statistical fluctuations and trivial charged–neutral fluctuations arising in generic particle production. Statistical fluctuations due to finite number effects and small data samples are studied by a comparison with mixed events generated from the data, as mentioned above. In addition, the magnitude of trivial charged–neutral fluctuations arising in generic particle production have also been studied with simulated events produced by the VENUS event generator [19] passed through the GEANT detector simulation [20] of the WA98 experiment setup, here referred to as VG events, and mixed events generated from these VG events. For this study, 27k VG simulated Pb + Pb collision events, corresponding to the 15% most central collisions of the data sample, have been generated with centrality selection provided by the MIRAC transverse energy [21].

Fig. 1 (top) shows the f distribution for data for the 5% most central Pb + Pb events within different regions of $\Delta\phi = 60°$ in an event. For comparison, the distribution obtained from M1 mixed events is also shown together with a Gaussian function fitted to the mixed event distribution. It is observed that the f distributions for the data and mixed events are asymmetric and extend beyond the Gaussian fit to larger f-values. In Fig. 1 (bottom) the ratio of the f distribution for the data to the Gaussian fit to the mixed event distribution is shown along with the ratio of the mixed event distribution to its Gaussian fit. The high value of the ratio at large f signifies vanishing small values of the fitted distribution. The f distribution for the data is observed to be broader than that of the mixed events with small and large f-values occurring more frequently. Because of the predominance of generic pion production around $f \approx 1/3$, non-statistical fluctuations can best be studied in the tail regions of the f distribution.

For this reason we focus our attention on the maximum and the minimum f-values (i.e., f_{max} and f_{min}) amongst all $\Delta\eta$–$\Delta\phi$ regions in each event in order to search for photon-excess and charge-excess type fluctuations. This is done using the SWM, where the azimuthal plane is scanned by sliding the $\Delta\phi$ window of chosen size in steps of $\delta\phi = 2°$ (limited by the azimuthal resolution of the SPMD) and computing f for each $\Delta\phi$ region to extract the maximum and the minimum values of f in each event, represented by f_{max} and f_{min}, respectively. The window size is kept fixed in η and varied in azimuth from $\Delta\phi = 20°$ to 150°. The f_{max} and f_{min} distributions for the experimental data and for VG events for the 5% most central Pb + Pb events are shown in Fig. 2 for a window size of $\Delta\phi = 60°$. The distributions for mixed events generated from data and VG events are also shown. The measured f_{max} and f_{min} distributions are seen to extend further to the right and left, respectively, than the mixed events distributions, with the difference observed in the data seen to be greater than that for the VG events.

In order to study the fluctuations in greater detail the mean (μ) and RMS deviation (σ) are calculated for the mixed event distributions for both the experimental data and the VG events separately because of differences in multiplicity distributions [17]. The events in the tails of the f_{max} and f_{min} distributions of the experimental data and the VG events are selected by applying a cut at $\mu \pm n\sigma$, with positive sign being applied for the f_{max} distribution and negative sign for the f_{min} distribution. Events having regions with f_{max} or f_{min} values beyond the cut are labeled as 'exotic' events. Results for n values of 3 and 4 are presented.

Fig. 3 displays a scatter plot of N_{ch} versus N_γ for a randomly selected $\Delta\phi = 60°$ region in each event. A weak correlation of N_{ch} with N_γ is observed due to residual impact parameter correlations, but with a wide spread. It is observed that a few points lie beyond the main cluster of events corresponding to events with large fluctuations in the multiplicities of photons and charged particles. When the SWM is applied to the same events to select those

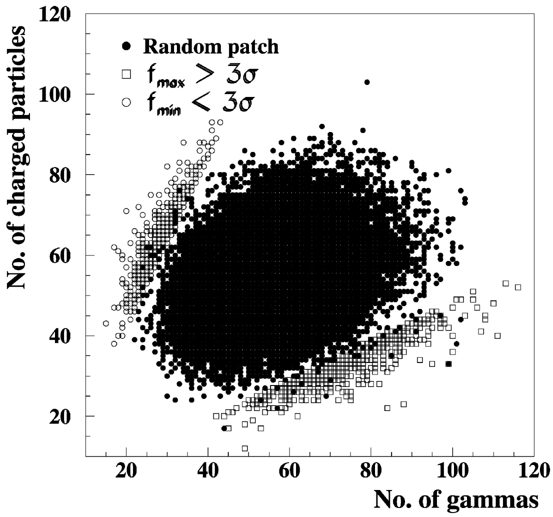

Fig. 3. Scatter plot of N_{ch} versus N_γ for a randomly selected 60° region for the 5% most central Pb + Pb events (solid points). The N_{ch} versus N_γ correlation for the photon and charge excess regions found by the SWM with the 3σ cut for the same event sample is also shown (open points).

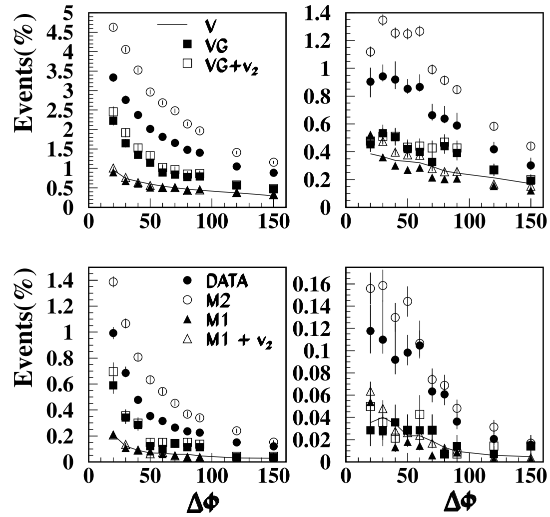

Fig. 5. Percentage of events having regions with f_{max} (left) exceeding 3σ (top) or 4σ (bottom) cuts and with f_{min} (right) less than 3σ (top) or 4σ (bottom) cuts versus $\Delta\phi$ for different sample types as described in the text.

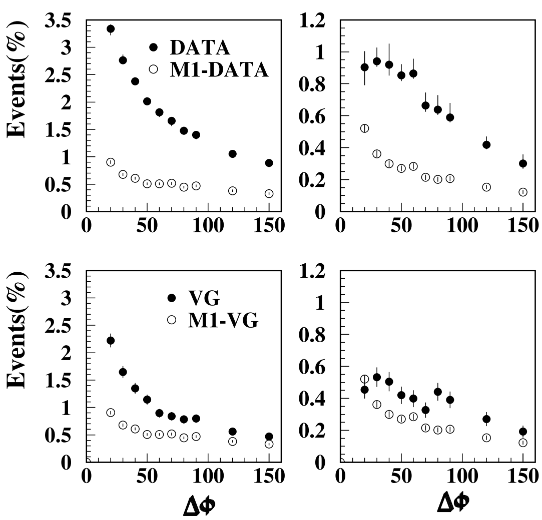

Fig. 4. The percentage of events having $\Delta\eta$–$\Delta\phi$ regions with f_{max} exceeding a 3σ cut (left) and with f_{min} less than a 3σ cut (right) versus the window size $\Delta\phi$ for the 5% most central events for data (top) and for VG (bottom) together with the results for their respective mixed events. Errors bars denote both statistical and systematic contributions.

events where the f values exceed $(\mu + 3\sigma)$ for f_{max} or fall below $(\mu - 3\sigma)$ for f_{min} many more events with regions having large fluctuations in the number of photons and charged particles are found, as shown by the open points in Fig. 3.

Fig. 4 shows the percentage of events beyond the $\mu \pm 3\sigma$ cut as a function of the window size $\Delta\phi$. Results are shown for data and mixed events in the top panel and for VG events and VG mixed events in the bottom panel. The results for the mixed events from data and VG are seen to be very similar. If the f_{max} (f_{min}) distributions were well described by a Gaussian function, the percentage of mixed events exceeding the 3σ cut is expected to be 0.135%, independent of $\Delta\phi$. Instead, it is observed that due to the asymmetry of the f_{max} (f_{min}) distribution (see Fig. 2) there are excess number of events in the region of larger (smaller) f-values, with an excess that grows with decreasing $\Delta\phi$ bin size, even for mixed events. It is observed that the percentage of exotic events in the data exceeds that in mixed events for all $\Delta\phi$ bin sizes for both the photon-excess and charge-excess selections. While the mixed events for data and VG events are very similar, the difference between data and mixed events exceeds the difference between VG and its mixed events. It is also seen that the difference between VG and its mixed events is much less for the charge-excess case than for the photon-excess case. The PMD-SPMD detector combination is better suited to study the photon-excess fluctuations because the purity of the photon sample in the PMD improves for large f and can reach values up to 85% [22]. For the charge-excess case the charged particle contamination plays a significant role in reducing the purity of the photon sample, which can be as low as 45%, and also introduces unwanted correlations due to charged hits in the SPMD that are simultaneously mis-identified as photon hits in the PMD.

The various sources of systematic errors associated with N_γ and N_{ch} distributions have been investigated and described in detail previously [17]. The systematic error in the determination of photon multiplicity is $(-7.1\%, +3.4\%)$ and in the charged multiplicity it is $\pm 4\%$. To investigate the systematic errors on the number of observed patches, a new set of event samples was generated by randomly (a) removing 7.1% of photon hits and adding 4% of charged particle hits and (b) adding 3.4% photon hits and removing 4% charged particle hits. For these samples mixed events samples were also generated. These new event samples were analyzed in the same way as the real data and mixed events samples mentioned earlier to obtain the systematic errors. Errors shown in figures are the quadratic sum of statistical and systematic errors.

The percentages of exotic events having photon and charge excess regions have been further investigated for additional types of event samples. In order to determine if the larger fluctuations observed in the data might be due to elliptic flow, the mixed and VG events have been modified by introducing elliptic flow following the method of Poskanzer and Voloshin [23]. The p_T dependent values of v_2 are taken from Ref. [24]. Since the p_T of the particles is not measured in the PMD or SPMD, a v_2 value has been assigned to a given particle following the p_T probability distribution obtained from the VENUS event generator. Fig. 5 (top) shows the percentage of events in which f_{max} (left) exceeds the 3σ cut or in which f_{min} (right) is less than the 3σ cut versus $\Delta\phi$ for M1 mixed events with flow (M1 + v_2) and VENUS + GEANT with flow (VG + v_2). It is seen that the observed enhancement in the per-

Table 1
Percentages of exotic events for the 4σ cut on the f_{max} (photon excess) or f_{min} (charge excess) for Data, M1 mixed, Venus + Geant (VG) and M2 mixed events for different centralities for the $\Delta\phi = 60°$ window size. The statistical and systematic errors are indicated.

Cent.	Sample	f_{max}	f_{min}
0–5%	DATA	0.316 ± 0.020	0.105 ± 0.012
	SYS ER	+0.005–0.015	+0.019–0.000
	M1	0.081 ± 0.010	0.014 ± 0.004
	VG	0.100 ± 0.027	0.028 ± 0.014
	M2	0.471 ± 0.027	0.083 ± 0.011
5–10%	DATA	0.260 ± 0.019	0.055 ± 0.009
	SYS ER	+0.016–0.006	+0.011–0.003
	M1	0.048 ± 0.008	0.013 ± 0.004
	VG	0.099 ± 0.033	0.000 ± 0.000
	M2	0.471 ± 0.028	0.113 ± 0.014
10–15%	DATA	0.274 ± 0.028	0.045 ± 0.011
	SYS ER	+0.023–0.020	+0.00–0.014
	M1	0.051 ± 0.0140	0.014 ± 0.007
	VG	0.074 ± 0.033	0.015 ± 0.015
	M2	0.357 ± 0.032	0.083 ± 0.016

centage of exotic events in the data cannot be explained as due to elliptic flow.

The analysis was also performed on M2 mixed events constructed as described above [11,12] by mixing the unaltered PMD hits of one event with the unaltered SPMD hits of a different event, keeping the same total number of photons and charged particles as in the original event, and hence keeping the overall correlation between them. The results for the M2 event analysis shown in Fig. 5 are seen to lie above the data signifying that the charged–neutral fluctuations in the data tend to be correlated and give rise less frequently to events with photon-excess or charge-excess regions than the randomly correlated charged and neutral hits of M2 mixed events. This behaviour was previously reported in Ref. [11] and is contrary to the naive expectations for a DCC. The result might be attributed to residual impact parameter correlations in the charged and neutral multiplicity in the data.

The curves shown in Fig. 5 were obtained from VENUS simulations without GEANT detector response for the 5% most central collisions corresponding to the impact parameter range 0–3.5 fm. The increase in the percentage of events with neutral or charge excess after application of the detector response (VG) is attributed to correlation due to detector effects where some charged particles may be mis-labeled as photons in the PMD.

The bottom panels of Fig. 5 show the same analysis as in the upper panels but with the cuts on the f_{max} (left) and f_{min} (right) distributions increased to 4σ. Although the percentage of events in the photon-excess or charge-excess regions are decreased with the more stringent cuts, as expected, the general trends and conclusions are the same when comparing the results for the 3σ cuts (Fig. 5 (top)) with those for the 4σ cuts (Fig. 5 (bottom)).

The analysis has also been performed for events in the 5–10% and 10–15% most central event selections. Table 1 compares these results for the 4σ cut with the 0–5% results for different event sample types as discussed above. This comparison shows little centrality dependence for the results over this limited range of centralities, there being a slight tendency of increased excess in the data with increasing centrality.

In addition to the event selection and data clean-up methods that have been employed, a set of additional checks have been performed with the 5% most central collisions for the $\Delta\phi = 60°$ window size to further examine the event structure and to search for possible detector artifacts.

The first check concerns the azimuthal distribution of the exotic regions. Fig. 6 (top) shows the azimuthal distribution of the center of the azimuthal window observed to contain an exotic photon or charge excess region. The regions are observed to be distributed throughout the full azimuth, indicating that the exotic regions are observed throughout the entire acceptance regions of the detectors.

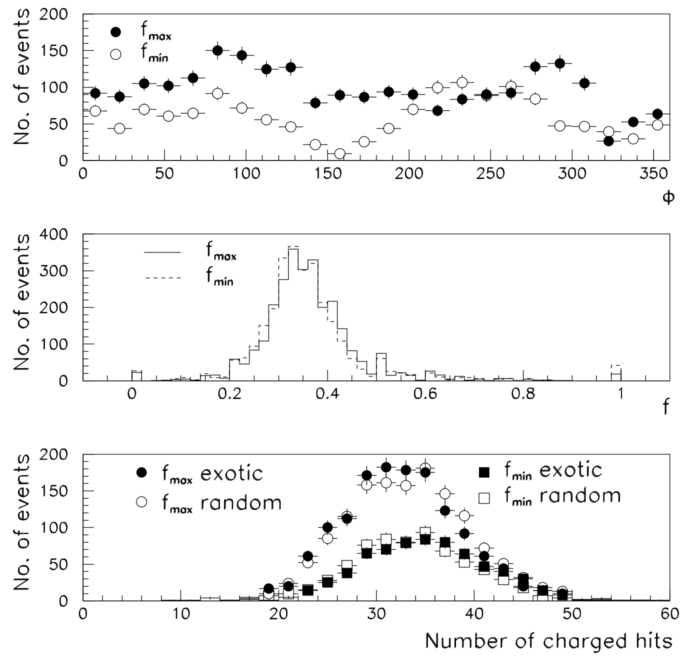

Fig. 6. Results of various checks: (top) azimuthal distributions of exotic photon and charge excess regions; (center) f distributions for preceding and succeeding events for the same region size at the same azimuth as indicated; and (bottom) charged particle multiplicity distribution in the non-overlapping η region of the SPMD at the same azimuthal position as the exotic region and in a randomly selected region of the SPMD of similar size in the same event.

The second check concerns the investigation of possible time-specific detector readout malfunctions. For each event found to have an exotic region, the neutral particle fraction (f) was calculated in the immediately preceding and immediately succeeding events in the same ($\Delta\eta, \Delta\phi$) region. The f distributions of these events associated to corresponding exotic events with f_{max} values exceeding the 3σ cut or f_{min} values less than the 3σ cut are shown in Fig. 6 (center). It is observed that the associated f distributions have their peak around 1/3 and exhibit behaviour similar to that of generic events, which in turn suggests normal detector operation.

The third check investigated the operation of the SPMD by examining if the observed variation in the number of charged particles in an exotic region extended to the pseudorapidity region $2.35 < \eta < 2.9$ of the SPMD that does not overlap with the PMD. Fig. 6 (bottom) compares the charged particle multiplicity distributions in the non-overlapping part of the SPMD in the same azimuthal zone as the exotic region, and in the same event, with the distributions in a randomly selected region of similar size, for photon excess as well as for charge excess regions. The good agreement of the charged particle multiplicity distributions for regions near the exotic location and random regions suggests normal operation of the SPMD when the exotic regions are found.

In summary, photons and charged particles have been measured in a common η–ϕ phase space region in the WA98 experiment for 158 A GeV Pb + Pb collisions. The results were analyzed for the 15% most central collisions to search for $\Delta\eta$–$\Delta\phi$ regions of photon or charged multiplicity excess using the sliding window method. The neutral particle fraction (f) has been calculated in $\Delta\eta$–$\Delta\phi$ regions within $2.9 < \eta < 3.75$ for different $\Delta\phi$ windows.

It is found that regions with photon or charged multiplicity excess occur more frequently in the data than in fully mixed events or in VENUS + GEANT simulation events. Comparison with minimally mixed events indicates that charged neutral fluctuation in the data tend to be correlated. The percentage of events with photon-excess or charge-excess increases with decreasing $\Delta\phi$ bin size, but varies little if at all as a function of centrality within the 15% most central collision event sample. The exotic regions having large charged–neutral fluctuations are distributed throughout the azimuthal acceptance. Several investigations have been performed to rule out possible detector artifacts. The comparison with the analysis of mixed events provides a model independent demonstration of non-statistical charged–neutral fluctuations. The comparison with VENUS suggests that these fluctuations are beyond those arising from generic particle production and decay.

Acknowledgements

We wish to thank the CERN accelerator division for the excellent performance of the SPS accelerator complex. We acknowledge with appreciation the effort of all engineers, technicians, and support staff who have participated in the construction of this experiment. This work was supported jointly by the German BMBF and DFG, the U.S. DOE, the Swedish NFR and FRN, the Dutch Stichting FOM, the Polish MEiN under Contract No. 1P03B02230 and CERN/88/2006 The Grant Agency of the Czech Republic under contract No. 202/95/0217, the Department of Atomic Energy, the Department of Science and Technology, the Council of Scientific and Industrial Research and the University Grants Commission of the Government of India, the Indo-FRG Exchange Program, the PPE division of CERN, the Swiss National Fund, the INTAS under Contract INTAS-97-0158, ORISE, Grant-in-Aid for Scientific Research (Specially Promoted Research & International Scientific Research) of the Ministry of Education, Science and Culture, the University of Tsukuba Special Research Projects, and the JSPS Research Fellowships for Young Scientists. ORNL is managed by UT-Battelle, LLC, for the U.S. DOE under contract DE-AC05-00OR22725. The MIT group has been supported by the U.S. Dept. of Energy under the cooperative agreement DE-FC02-94ER40818.

References

[1] B. Mohanty, J. Serreau, Phys. Rep. 414 (2005) 263, and references therein.
[2] J.-P. Blaizot, A. Krzywicki, Phys. Rev. D 46 (1992) 246.
[3] C.M.G. Lattes, et al., JACEE Collaboration, Phys. Rep. 65 (1980) 151.
[4] M.V.S. Rao, D0 Collaboration, Fermilab-CONF-94-343-E, Sept. 1994.
[5] P.L. Melese, CDF Collaboration, Fermilab-CONF-96-205-E, July 1996.
[6] T.C. Brooks, et al., MINIMAX Collaboration, Phys. Rev. D 61 (2000) 032003.
[7] H. Appelshäuser, et al., NA49 Collaboration, Phys. Lett. B 459 (1999) 679.
[8] W.T. Lin, et al., Nucl. Instr. Meth. Phys. Res. A 389 (1997) 415.
[9] M.M. Aggarwal, et al., Nucl. Instr. Meth. Phys. Res. A 424 (1999) 395.
[10] M.M. Aggarwal, et al., WA98 Collaboration, Phys. Lett. B 420 (1998) 169.
[11] M.M. Aggarwal, et al., WA98 Collaboration, Phys. Rev. C 64 (2001) 011901R.
[12] M.M. Aggarwal, et al., WA98 Collaboration, Phys. Rev. C 67 (2003) 044901.
[13] M.M. Aggarwal, G. Sood, Y.P. Viyogi, Phys. Lett. B 638 (2006) 39.
[14] B.K. Nandi, et al., Phys. Lett. B 461 (1999) 142.
[15] Gopika Sood, PhD Thesis, Panjab University, Chandigarh, 2002.
[16] M.M. Aggarwal, et al., WA98 Collaboration, Pramana 60 (2003) 987.
[17] M.M. Aggarwal, et al., WA98 Collaboration, Phys. Lett. B 458 (1999) 422.
[18] T.C. Awes, et al., Nucl. Instr. Meth. A 279 (1989) 479.
[19] K. Werner, Phys. Rep. 232 (1993) 87.
[20] R. Brun, et al., GEANT3 user's guide, CERN/DD/EE/84-1, 1984.
[21] M.M. Aggarwal, et al., WA98 Collaboration, Phys. Rev. C 65 (2002) 054912.
[22] B. Mohanty, T.K. Nayak, Y.P. Viyogi, D.P. Mahapatra, Int. J. Mod. Phys. A 19 (2004) 1453.
[23] A.M. Poskanzer, S.A. Voloshin, Phys. Rev. C 58 (1998) 1671.
[24] C. Alt, et al., NA49 Collaboration, Phys. Rev. C 75 (2007) 044901.